In situ optical observations of keyhole dynamics during laser drilling

Meng Chen, Yuren Wang, Gang Yu, Ding Lan, and Zhongyu Zheng

Re-register for Table of Content Alerts
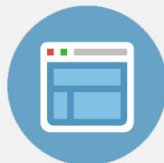
Create a profile. Sign up today!

In situ optical observations of keyhole dynamics during laser drilling

Meng Chen,[1] Yuren Wang,[1,a)] Gang Yu,[2,b)] Ding Lan,[1] and Zhongyu Zheng[1]

[1]*Key Laboratory of Microgravity, Institute of Mechanics, Chinese Academy of Sciences, Beijing 100190, People's Republic of China*
[2]*Key Laboratory of Mechanics in Advanced Manufacturing, Institute of Mechanics, Chinese Academy of Sciences, Beijing 100190, People's Republic of China*

To better understand the laser drilling process and especially to clarify keyhole dynamics in metal drilling, a quasi-two-dimensional drilling assembly was set up with a thin sandwich structure. Keyhole dynamics coupling multiple physical processes were recorded using high-speed photography, and clear images were obtained. The formation of keyholes was found not to be a single unified process, and the whole drilling process could be divided into five stages: an initial melt ejection, mild melting, rapid drilling, hole expansion, and backflow and recasting. As the keyhole evolved, the removal of material changed. © 2013 AIP Publishing LLC.
[http://dx.doi.org/10.1063/1.4829147]

Because of continuously growing demand for precision machining, laser micromachining—especially laser drilling—is extensively employed in advanced manufacturing such as microhole machining.[1–3] Laser drilling is the process by which a high-power laser beam is focused onto a workpiece to melt and vaporize the material to create a hole.[4] A deep and narrow cavity in the molten pool, known as a "keyhole," is created by the recoil pressure associated with energetic evaporation during the drilling process.[5] Owing to the narrow concave shape of the keyhole, the energy concentrated at the bottom of the melt pool results in deeper penetration of the laser beam and higher efficiencies for laser drilling.[6,7] In rapid laser drilling, keyhole formation is an unstable process. Although much has been performed to explain the mechanism of formation, the keyhole instability is far from being completely understood.[5–12] Multiple physical processes are involved in the millisecond laser drilling process which couples keyhole dynamics with melt flow, melt pool boiling, plasma generation inside the drilling hole, and melt droplet ejection and evaporation outside the drilling hole.[13–18] The complexity and intricacy of these processes pose an obstacle to a comprehensive understanding of keyhole instability and especially to explain its evolution.

Direct optical observation is often used to obtain *in situ* observations of laser machining processes.[12,18–21] High-speed photography was developed to observe exterior phenomena such as surface morphology of the keyhole and melt droplet ejection.[18,19] Optical observations of interior phenomena were only performed for transparent materials such as sugar-based materials and soda lime glass.[20–23] Obviously, the dynamic processes observed in these model materials need strict restrictions to be transferred into real processes in metallic workpieces simply because physical and thermal properties differ greatly.[23] In another development, X-ray radiography was recently used to study keyhole dynamics, but its temporal resolution and X-ray contrast of the vapor phase were very low.[24] Thus it is impossible to detect and trace ejections and evaporations from X-ray photography. Up to now, because of the lack of an effective means to detect all of the physical processes in laser drilling, no sufficient solid proof has been obtained to reveal the dynamics during laser drilling or keyhole evolution.

Rapid temporal changes and opacity of metals are the main obstacles in optical observations of the dynamic processes. In addition, strong plasma, excited by the high-density laser beam, overexposes data recordings and obscures contrast differences between plasma and melt in images. To solve these problems, an *in situ* optical observation assembly recording a quasi-two-dimensional (2D) laser drilling metal process was proposed. A schematic setup of the experiment is shown in Fig. 1. The sample cell possesses a sandwich structure (glass-metal-glass). Both sides of metal plate were covered with an optical transparent glass plate. The two glass plates were used as transparent walls and provided constrain to the melt in drilling process. A molybdenum plate was selected for the study because of its high melting and boiling points. Compared with other metals, the temperature difference between plasma and molybdenum melt was relatively small. The advantage of this was that the radiation brightness difference between both these states could be effectively
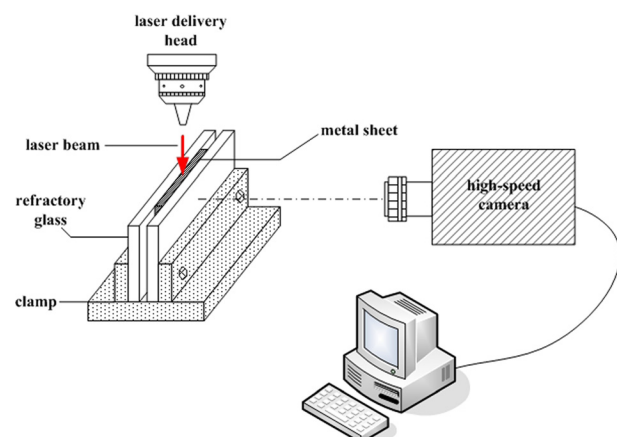

FIG. 1. Schematic diagram of assembly and experiment setup.

a)Electronic mail: yurenwang@imech.ac.cn
b)Electronic mail: gyu@imech.ac.cn

reduced, and clear plasma images and melt images can then be simultaneously obtained. Considering both the visualization of the melt flow and similarity with the real drilling process, the thickness of the molybdenum plate was rigidly controlled to be slightly thicker than the diameter of the laser beam. So the whole drilling process was considered to be a quasi-two-dimensional (2D) laser drilling process. The shutter speed and aperture size were also optimized to avoid image overexposure. With this assembly, the dynamic laser drilling process was recorded in real time. Developments within the drilling hole could be clearly observed.

A Nd:YAG solid continuous laser system was used at the operating wavelength of 1.064 μm. The focal plane of the beam was set slightly above the sample surface by 150 mm condenser lens. The spot size was approximately 0.11 mm. A blind hole was drilled using a single laser pulse without shielding gas. The high speed imaging system without contrast illumination was used to capture the drilling process. The camera was placed about 200 mm from the side of the workpiece and faced towards the drilling area. The recording rate was 100 000 f/s at a resolution of 192 × 192 pixels or 50 000 f/s at 256 × 312 pixels. The shutter speed was set at 1/2 700 000 s or 1/1 000 000 s.

The physical processes in laser drilling are similar at different conditions of the high density laser pulse. The drilling process using a signal laser pulse with pulse width of 10 ms and an average power of 1000 W was took for an example as shown in Fig. 2. The images at different laser conditions are shown in supplementary material.[25] Sequential images of the drilling hole from a single-pulse laser beam (Fig. 2(a)) show that keyhole evolution can be clearly seen forming and evolving in the drilling hole. One-pixel wide streaks, running vertically through the hole center, were abstracted from all 1800 frames over the single-pulse duration. The streaks were then merged to form Fig. 2(b). In this manner, the drilling rate of the hole could be obtained quantitatively. Using hole configuration and drilling rate, the whole drilling process can be divided into five stages: (I) the initial melt ejection, (II) mild melt melting, (III) rapid drilling, (IV) hole expansion, and (V) backflow and recasting.

When the high-power pulsed laser irradiates the sample surface in stage I (see Fig. 2(a)), the instantaneous temperature of the metal surface exceeds by far the metal boiling point. Melting and vaporization occur simultaneously. The first appearance of vapor (Fig. 2(a), I) establishes the initial time of 0 ms. Almost at the same time (a delay of just 0.02 ms), a thin molten layer forms beneath the sample surface. Because of the recoil pressure induced by vaporization and the Marangoni shear force induced by surface tension gradients, the radial melt flow in the melt pool forms the initial melt ejection. After about 0.04 ms, a large number of metal droplets with sizes of several to several tens of microns spray outward at velocities of several meters per second (as shown in Fig. 2(c)). These velocities are comparable to the ones as mentioned in previous works, where the ejection was assumed as a sudden release of liquid material when the surface tension forces were overcome by the pressure gradients.[26] Because melt is being ejected from the melt pool, the keyhole has not formed in stage I. After 0.4 ms, a pit forms in the sample surface, and the initial melt ejection stops. In this stage, ejections dominate material removal.

After the initial ejections, the recoil pressure is not sufficiently large to overcome the surface tension of the melt and expel melt from the hole.[27] Hence, the ejections stop for a while, laser drilling passes into a mild melt melting stage which lasts about 3 ms. In this stage, most of the energy is used to melt more solid material, and the melt front rapidly expands to lower depths (Fig. 2(a), II). In the absence of ejections, surface evaporation became the main way for material removal. Because the recoil pressure is low, the keyhole is shallow. The melt flow driven by temperature gradients can be clearly seen in this process.

In stage III, after 3.1 ms, the melt pool begins to boil as temperature increases. The evolution of keyhole and melt flow is clearly observed (Fig. 2(a), III). A narrow but deep keyhole is produced beneath the surface of the melt pool (Fig. 2(d)), and the melt front rapidly spreads to greater depths. There are dazzling light spots at the bottom of the drilling hole, and spatters reappear outside the drilling hole. From the violent vaporization during boiling, a high recoil pressure acts on the surface of the melt pool to produce the keyhole which acts as a waveguide for the incident laser beam. Multiple light reflections on its wall enable the beam to propagate down to the bottom of the hole, where the brightness of the light reaches its maximum.[28] This results in an increase in the total energy transfer rate from laser to
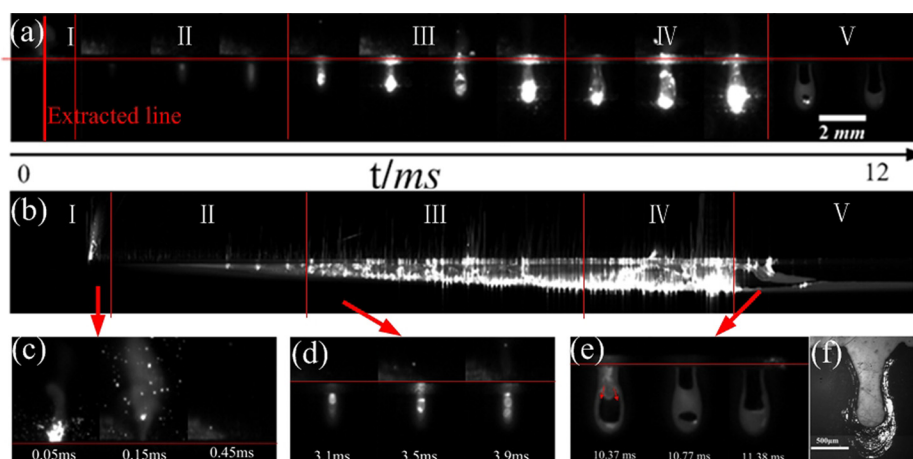

FIG. 2. Thirteen time-series images at 1 ms intervals (a) and streak photographs (b) of the whole drilling process, which include initial melt ejections (c), rapid drilling (d), reflux and recasting (e), where each image has a resolution of 192 × 192 pixels at a recording rate of 100 000 f/s, and an optical photo of the drilled hole (f).

material. A high drilling rate (Fig. 2(b), III) is obtained through this effect of the keyhole, called keyholing. In this stage, although vaporization and ejections are both occurring, the mechanisms underlying these processes have changed fundamentally as beam absorption increases.

In contrast, the vaporization mechanism in stage III has converted from surface evaporation to volume vaporization in the form of boiling. The vaporization model for a high-density laser drilling process given in previous work suggested these two different mechanisms.[23,29,30] However, there are still lacks of visual evidences verified the existence of boiling during metal drilling. Visual evidence for boiling is given here with regard to two aspects. First, the area changes in the dazzling light-spots in the bottom of the drilling hole (Fig. 2(a), III) imply a more violent evaporation than normally occurs with surface evaporation, i.e., explosive boiling after 3.1 ms. Second, bubbles during boiling were captured after the laser pulse stopped (Fig. 3(a)). To clarify the model of vaporization, the high-speed imaging system was optimized to observe in greater detail this phenomenon occurring in the melt pool. At the end of the laser drilling process, bubbles were observed to nucleate in the molten pool, then to expand and merge, and finally to burst at the metal surface (Fig. 3(a)). The appearance of the bubbles suggests that the melt is still above boiling point shortly after the laser pulse ends. The light captured by the camera is all from blackbody radiation, so the gray-scale of the images can be used to characterize the temperature field. Color images are generated using pseudo-color processing to highlight the temperature field; Fig. 3(b) shows clearly that the highest temperature is at the surface where the bubbles burst. Bubbles in the melt pool after laser irradiation indicate that a violent, or explosive, boiling occurs during drilling. The explosive boiling caused by the concentrated energy through keyholing is a very efficient way for removing material.

The mechanisms for spatter formation are different from those for ejection in stage I. The melt flew radially outward from the melt pool forming the initial burst of ejections attributed to radial pressure gradients whereas spatters in stage III are induced by explosive boiling.[13] Under the enormous recoil pressure, the boiling melt flies upwards to the hole exit and bursts into droplets at the surface. Compared
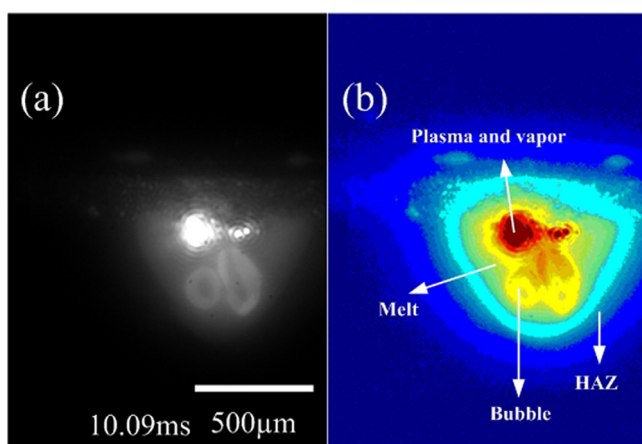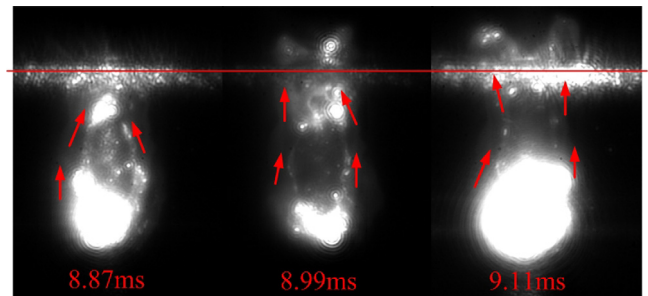

FIG. 4. High-speed images of melt flow inside the hole; the resolution is 256×312 pixels at a recording rate of 50 000 f/s and shutter speed of 1/2 700 000 s.

with initial ejections, the larger spatters in rapid drilling move slower and their number largely decreases. Both explosive boiling and ejection occur in this process, with boiling playing the leading role in material removal.

In keyhole evolution, ionized vapor as plasma fills the keyhole and acts as a shield to block laser-energy transfer, thus widening the hole (Fig. 2(a), IV).[31] The melt driven by the recoil pressure climbs the hole wall and accumulates at the hole exit (see Fig. 4). The diameter of the hole is seen to be enlarged whereas the depth of the hole has not substantially changed (Fig. 2(a), IV); the drilling rate (Fig. 2(b), IV) decreases sharply. An interesting phenomenon was noted in which turbulence was occurring in the dazzling area in the bottom of the hole (see Fig. 4). This phenomenon suggests that the keyhole is unstable. Energy is being trapped in the melt pool because of plasma shielding, resulting in explosive boiling and oscillations in the melt pool. From the turbulence of the process, the shape of the keyhole would continuously change. This instability coupled with melt pool oscillations causes irregularities in the energy absorption at the liquid/vapor interface. Meanwhile, because of the inverse bremsstrahlung process and Fresnel absorption, the laser energy tends to concentrate on the keyhole wall, rather than at the bottom.[31] The concentrated energy is rapidly transmitted to the surrounding solid by the upward flow of melt. This results in the solid-liquid interface developing laterally, and the drilling rate decreases during this hole expansion. Both mechanisms for material removal are active in this process with vaporization dominating.

After laser irradiation, the drilling process passes to a backflow and recasting stage (Fig. 2(a), V). The melt accumulated in the exit of the drilling hole flows back to fill the keyhole, and a part of the hole is sealed with refilled melt (Fig. 2(e)). The high-temperature melt keeps boiling for a short time and finally solidifies. The shape of the final hole (Fig. 2(f)) is different from the hole observed during drilling. The reflux changes the geometry of the drilling hole and reduces the reproducibility of the final hole shape.

In summary, this work provided clear images using a quasi-2D assembly to observe laser metal drilling that enabled detailed descriptions of its dynamic processes. Keyhole formation was not uniform, and the whole drilling process divides into five stages: initial melt ejection, mild melt melting, rapid drilling, hole expansion, and backflow and recasting. During rapid drilling, the keyhole rapidly spreads deeper because energy is channeled to the bottom of

FIG. 3. Gray-scale (a) and pseudo-color images (b) after the interaction; the resolution is 256×312 pixels with a recording rate of 50 000 f/s and shutter speed of 1/1 000 000 s.

the hole through keyholing. In addition, effective material removal from explosive boiling occurs as energy absorption increases. Keyhole instability and unique hole expansions are observed in stage IV. The diameter of the hole is enlarged, and the drilling rate decreases in this process due to plasma shielding and melt flow. In the final stage, the melt accumulating at the exit of the drilling hole flows back to refill the keyhole; the drilled hole is reshaped from its form during rapid drilling. Our work revealed the keyhole dynamics in the rapid drilling process and provides some theoretical guidance to processes occurring in real laser metal drilling.

[1]C. Y. Yeo, S. C. Tam, S. Jana, and M. W. S. Lau, J. Mater. Process. Technol. **42**, 15 (1994).

[2]M. D. Shirk and P. A. Molian, J. Laser Appl. **10**, 18 (1998).

[3]A. K. Nath, D. Hansdah, S. Roy, and A. R. Choudhury, J. Appl. Phys. **107**, 123103 (2010).

[4]Y. Zhang and A. Faghri, Int. J. Heat Mass. Transfer **42**, 1775 (1999).

[5]J. Y. Lee, S. H. Ko, D. F. Farson, and C. D. Yoo, J. Phys. D: Appl. Phys. **35**, 1570 (2002).

[6]H. Ki, P. S. Mohanty, and J. Mazumder, J. Laser Appl. **14**, 39 (2002).

[7]K. W. Park and S. J. Na, Appl. Surf. Sci. **256**, 2392 (2010).

[8]P. Solana and G. Negro, J. Phys. D: Appl. Phys. **30**, 3216 (1997).

[9]J. H. Cho and S. J. Na, J. Phys. D: Appl. Phys. **39**, 5372 (2006).

[10]A. Matsunawa, J. D. Kim, N. Seto, M. Mizutani, and S. Katayama, J. Laser Appl. **10**, 247 (1998).

[11]V. V. Semak, G. A. Knorovsky, D. O. MacCallum, and R. A. Roach, J. Phys. D: Appl. Phys. **39**, 590 (2006).

[12]Y. Zhang, S. Li, G. Chen, and J. Mazumder, Opt. Laser Technol. **48**, 405 (2013).

[13]B. S. Yilbas and M. Sami, J. Phys. D: Appl. Phys. **30**, 1996 (1997).

[14]Q. Lu, S. S. Mao, X. Mao, and R. E. Russo, Appl. Phys. Lett. **80**, 3072 (2002).

[15]M. Brajdic, M. Hermans, A. Horn, and I. Kelbassa, Meas. Sci. Technol. **19**, 105703 (2008).

[16]J. J. Chang and B. E. Warner, Appl. Phys. Lett. **69**, 473 (1996).

[17]H. Ki, J. Appl. Phys. **107**, 104908 (2010).

[18]K. T. Voisey, S. S. Kudesia, W. S. O. Rodden, D. P. Hand, J. D. C. Jones, and T. W. Clyne, Mater. Sci. Eng. A **356**, 414 (2003).

[19]I. Eriksson, P. Gren, J. Powell, and A. F. H. Kaplan, Opt. Eng. **49**, 100503 (2010).

[20]D. K. Y. Low and L. Li, Opt. Laser Technol. **33**, 515 (2001).

[21]S. Döring, S. Richter, S. Nolte, and A. Tünnermann, Opt. Express **18**, 20395 (2010).

[22]X. Jin and L. Li, Opt. Laser. Eng. **41**, 779 (2004).

[23]A. Riveiro, F. Quintero, F. Lusquiños, R. Comesaña, and J. Pou, J. Phys. D: Appl. Phys. **44**, 135501 (2011).

[24]F. Abt, M. Boley, R. Weber, T. Graf, G. Popko, and S. Nau, Phys. Proc. **12**, 761 (2011).

[25]See supplementary material at http://dx.doi.org/10.1063/1.4829147 for images of different laser conditions.

[26]P. Solana, P. Kapadia, J. Dowden, W. S. O. Rodden, S. S. Kudesia, D. P. Hand, and J. D. C. Jones, Opt. Commun. **191**, 97 (2001).

[27]A. Matsunawa and V. Semak, J. Phys. D: Appl. Phys. **30**(5), 798 (1997).

[28]S. Fujinaga, H. Takenaka, T. Narikiyo, S. Katayama, and A. Matsunawa, J. Phys. D: Appl. Phys. **33**, 492 (2000).

[29]A. Miotello and R. Kelly, Appl. Phys. A: Mater. Sci. Process. **69**, S67 (1999).

[30]N. M. Bulgakova and A. V. Bulgakov, Appl. Phys. A **73**, 199 (2001).

[31]S. Sankaranarayanan, H. Emminger, and A. Kar, J. Phys. D: Appl. Phys. **32**, 1605 (1999).